CHAPTER 3

In vitro controlled release study of drug (Aspirin, Captopril and Camptothecin) from MCM-41 and TPA-MCM-41

Materials Science & Engineering C 98 (2019) 1014–1021

Contents lists available at ScienceDirect

Materials Science & Engineering C

journal homepage: www.elsevier.com/locate/msec

Camptothecin encapsulated into functionalized MCM-41: In vitro release study, cytotoxicity and kinetics

Priyanka Solanki[a], Shweta Patel[b], Ranjitsinh Devkar[b], Anjali Patel[a,*]

[a] Department of Chemistry, Faculty of Science, The Maharaja Sayajirao University of Baroda, Vadodara 390002, Gujarat, India
[b] Department of Zoology, Faculty of Science, The Maharaja Sayajirao University of Baroda, Vadodara 390002, Gujarat, India

ARTICLE INFO

Keywords:
MCM-41
12-tungstophosphoric acid
Camptothecin
In vitro release
MTT assay
Kinetics

ABSTRACT

The application of MCM-41 functionalized by 12-tungstophosphoric acid (TPA) as drug carrier for cancer treatment was studied by loading of camptothecin (CPT). In-vitro controlled release study of CPT in Simulated Body Fluid (pH 7.4, 37 °C) was carried out under stirring as well as static conditions. The systems were also evaluated on cancer cells (HepG2) and the carriers are found to be non-toxic to the cancer cells. In order to see the influence of inorganic moiety on release rate of drug, study was also carried out with CPT loaded unfunctionalized MCM-41. A detailed study on release kinetics and release mechanism using First Order Release Kinetic Model, Higuchi Model, Koresmeyer-Pepps Model and Extended kinetic model was also carried out.

1. Introduction

Camptothecin (CPT) is a naturally occurring quinolone alkaloid which shows significant anticancer activity with a broad spectrum of human malignancies and CPT is an inhibitor of the DNA-replicating enzyme topoisomerase-I [1]. Unfortunately, the clinical application of CPT is hindered by its poor pharmaceutical profile, with extreme aqueous insolubility, low stability of the lactone form at physiological pH, and severe systemic toxicities which included myelosuppression, vomiting, diarrhoea, and hemorrhagic cystitis [2–4]. A better understanding of mode of action, chemistry and pharmacology of the CPT led to the development of water-soluble derivatives such as irinotecan, topotecan and 9-aminocamptothecin [5]. Although less active than the CPT [6], these derivatives have gained approval by the Food and Drug Administration (FDA) for treating cancers. However, these CPT derivatives still suffer from important drawbacks mainly related to the poor stability of the lactone ring, the short half-life of the compounds in blood and a number of non-resolved toxic effects. Therefore, the development of controlled delivery strategies could lead to significant advantages in the clinical use of these drugs. In this sense, CPT has been encapsulated in different vehicles, like PLGA microspheres [7], solid lipid nanoparticles [8], liposomes [9] and micelles [10]. Reports are also available for camptothecin loading and release using functionalized as well as non-functionalized Silica nanoparticles [11] and polymeric nanoparticles [12]. Further, to modulate the release rate of CPT, carriers are functionalized by various organic molecules such as silica nanoparticles functionalized by 3-Mercaptopropl group [13] and Nucleic acids [14]. Functionalization leads to overcome the mentioned problems faced by CPT.

A literature survey shows that the functionalization was carried out using organic moiety only. It also shows that no reports are found on release study of CPT using either non-functionalized MCM-41 or functionalized MCM-41. In 1992, Mobil Corporation have synthesized the mesoporous silica materials and called as MCM-41. These are amorphous inorganic materials consisting of silicon and oxygen in their framework. Its pore sizes are in range of 2–50 nm in dimension. This material has been widely used as carrier as having unique characteristic such as ordered porosity at the mesoscale, variable pore size, high specific surface area, high adsorption capacity, high concentration of surface Si-OH groups through which it can interact with different functional group of drug. Hence, it was thought of interest to use combination of an inorganic moiety as a functionalizing agent and MCM-41 as new drug delivery systems. The idea was further motivated by recently published result by our group [15] where we have reported functionalisation of MCM-41 (pore diameter: 3.7 nm) by an inorganic moiety, 12-tungstophosphoric acids (TPA) and its use for the in vitro release of L-arginine where we found the beneficial effect of TPA and that encourage us to continue the work.

So, as an extension of our work, for the first time, we describe use of MCM-41 with different pore diameter (4.9 nm) as carrier for CPT. The present article describes functionalization of MCM-41 (pore diameter: 4.9 nm) by TPA, encapsulation of CPT and characterization using

* Corresponding author.
E-mail address: anjali.patel-chem@msubaroda.ac.in (A. Patel).

https://doi.org/10.1016/j.msec.2019.01.065
Received 22 June 2018; Received in revised form 4 January 2019; Accepted 15 January 2019
Available online 16 January 2019

Introduction

Water-soluble drug Captopril (Cap) is an orally active inhibitor of angiotensin-converting enzyme (ACE), having size of 9.0 × 5.7 × 3.3 A^o which has been widely used for the treatment of hypertension and congestive heart failure. It acts by inhibiting the active sites of the ACE, blocking the conversion of angiotensin I to angiotensin II. According to the Biopharmaceutical Classification System (BCS), Captopril is classified as a class III drug with high solubility and poor permeability. It is used for controlling blood pressure, treating heart failure, preventing cardiac remodeling and left ventricular dysfunction after myocardial infarction, and preventing kidney damage in people with hypertension or diabetes. It is one of the best documented ACE inhibitors [1-3]. However, instability of this drug due to its active functional group, thiol is the main drawback of its oral administration. Further, duration of drug in vivo requires long drug activity. These are the major drawbacks of oral administration of Captopril [4, 5]. Thus, release of Captopril can be studied using some carrier which can release it in controlled manner and protect it from degradation due to its active thiol group.

Various groups have studied release study of Captopril using different carrier functionalized by various organic moieties. Shilun Qiu et al have reported release of captopril from MCM-41 with different pore size [6]. Popovici et al have reported interaction of captopril and SBA-15 [7]. Shougui Li et al. have reported controlled release of captopril from MCM-41 functionalized by trimethylsilane [8]. Popovici et al have reported controlled release of captopril from SBA-15 functionalized by 3-aminopropyl group [9]. Recently, in 2019, Talker and his group have studied the permeability of Captopril using self-nanoemulsifying drug carrier [10].

Aspirin is a non-steroidal anti-inflammatory drug which acts by inhibiting the enzyme cyclooxygenase [11]. It is primarily used for the treatment of cardiovascular diseases [12] and also for analgesic and antipyretic effects [13]. Because of its shorter biological half-life and poor solubility it shows poor pharmacological profile [12, 14]. The administration of most anti-inflammatory drugs in therapeutic doses can lead to development of gastrointestinal inflammation or ulcers [15]. To avoid these problems, encapsulation of this anti-inflammatory drug, Aspirin, into various drug carriers have been attempted to achieve the desired goals.

Various groups have studied release study of Aspirin using different carrier functionalized by various organic moieties. Qian et al have reported MCM-41 modified by organic aminopropyl groups and used as carrier to deliver Aspirin [16]. Sun et al. have reported bimodal mesoporous silica functionalized by 3-aminopropyltriethoxysilane and studied the release of Aspirin [17]. Larsen et al., have reported loading and release of Aspirin from MCM-41 functionalized by Aminopropyl group [18]. Experimental and computational study of Aspirin loading and release from Zeolite HY was also reported by Larsen et al. [19]. Recently in 2019, various group have reported controlled release of Aspirin using thermosensitive hydrogel [20], magnetic nanoparticles [21], chitosan, metolose, and carrageenan based carrier [22] as well as lignin, a natural polymer [23].

Camptothecin (CPT) is an anticancer agent with a broad spectrum of human malignancies and is an inhibitor of the DNA-replicating enzyme topoisomerase-I [24]. Unfortunately, the clinical application of CPT is hindered by its poor pharmaceutical profile, with extreme aqueous insolubility, low stability of the lactone form at physiological pH, and severe systemic toxicities which included myelosuppression, vomiting, diarrhoea, and hemorrhagic cystitis [25-27]. Therefore, the development of controlled delivery strategies could lead to significant advantages in the clinical use of these drugs. In this sense, CPT has been encapsulated in different vehicles, like PLGA microspheres [28], solid lipid nanoparticles [29], liposomes [30] and micelles [31]. Reports are also available for CPT loading and release using functionalized as well as non-functionalized Silica nanoparticles [32] and polymeric nanoparticles [33]. Further, to modulate the release rate of CPT, carriers are functionalized by various organic molecules such as silica nanoparticles functionalized by 3-Mercaptopropl group [34] and Nucleic acids [35]. Since 2018, various group have reported controlled release of Camptothecin using Polyphosphoramidate nanoparticles [36], graphene oxide nanoparticle functionalized with polyethylene glycol and folic acid [37], polylactide [38], poly(L-glutamic acid)-graft-methoxy poly(ethylene glycol) [39], poly(2-hydroxyethyl methacrylate) nanoparticles [40], lipid base nanoparticles [41], Folic acid-conjugated chitosan [42], graphene oxide nanoparticle functionalized with polyethylene glycol and folic acid [43], pegylated polyelectrolyte nanocarriers [44], organophosphorous derivatives-chitosan hydrogel [45], poly(lactic-co-glycolic)acid microspheres [46], magnetic iron oxide nanoparticles [47], Amino modified metal-

organic frameworks [48] and Testosterone- and vitamin-grafted cellulose ethers [49] as carrier.

Literature survey shows that TPA-MCM-41 has never been reported as carrier for delivery of Captopril, Aspirin and Camptothecin. This chapter describes the in vitro controlled release of Captopril, Aspirin and Camptothecin from MCM-41 and Functionalized MCM-41. Release study of selected drugs have been carried out at different pH (7.4 and 1.2) as well as under stirring and static condition. Further, comparisons of release profile of drug loaded materials and physical mixture of drug-carrier has been included. To examine the Captopril release kinetic and mechanism, first order release kinetic model and Higuchi model has been used. Further, kinetic and mechanism of Aspirin and Camptothecin release was also carried out using same model with addition of two more model (Korsmeyer-Peppas model (KPM) and Extended Kinetic model (EKM)). Captopril release data did not fit with KPM and EKM and hence, is not included into the chapter.

EXPERIMENTAL

In vitro controlled release of Captopril

Preparation of Calibration curve for Captopril

Stock solution of Captopril was prepared by dissolving 10 mg in 100 ml SBF. From this stalk solution 15-35 µg/mL solutions were prepared by diluting specific quantities of the stalk solution using SBF mixture. The absorption of prepared solutions were taken at 203 nm wavelength using Perkin Elmer UV-Visible spectrophotometer. Using same method, working curve was also obtained for SGF also (Figure 1)

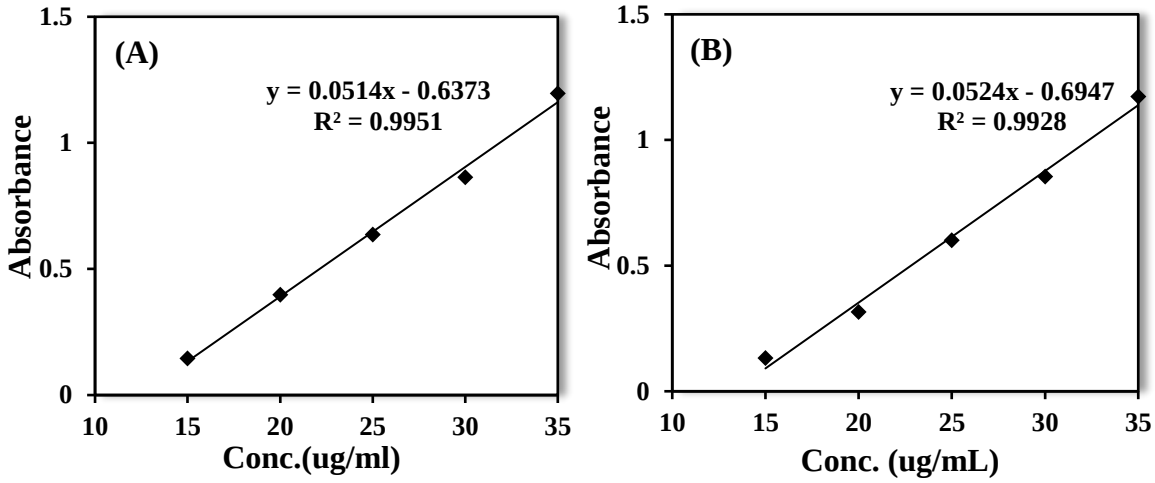

Figure 1. Calibration curve of Captopril in (A) SBF (pH 7.4) and in (B) SGF (pH 1.2)

(a) In vitro release of Captopril

In vitro release of Captopril was obtained by soaking drug loaded materials (Cap/MCM-41 and Cap/TPA-MCM-41) in 100 mL of SBF at 200 rpm at 37 ^{o}C temperature. At proper time interval, 1 mL of release fluid was taken and fresh SBF was added to maintain the constant volume of the system. The 1 mL fraction was diluted and analyzed for Captopril content using UV-Visible spectrophotometry at 302 nm. All the experiments were repeated three times. Similarly, release study was also carried out in simulated gastric fluid (SGF) (pH 1.2) also.

Results and discussion

(i) Comparison with Physical mixture

In order to see whether the Captopril molecule is only physically adsorbed on the outer surface of carrier or not, release profile of Captopril loaded material and physical mixture of Captopril and carrier was compared and shown in Figure 2.

It is clear from the Figure 2 that physical mixture shows 100% dissolution of Captopril within 1 h while Captopril loaded material shows controlled and ordered release which suggests the presence of drug molecule inside the channel of carrier. This is already confirmed by BET surface area analysis.

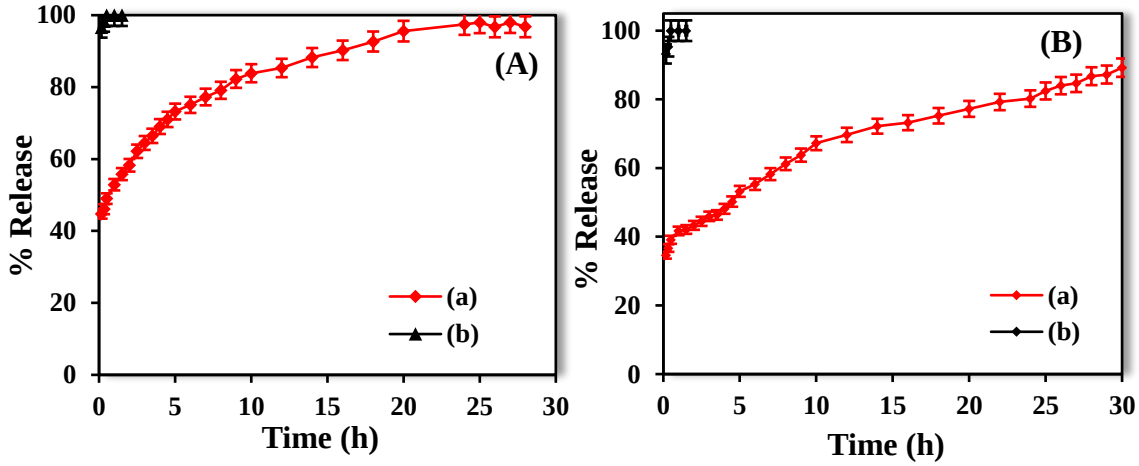

Figure 2. Comparison of release profile of (A) **a** Cap/MCM-41 and (B) **a** Cap/TPA-MCM-41 with **b** physical mixture

(ii) Effect of stirring on release rate of Captopril

To investigate the effect of stirring on release rate of Captopril, in vitro release study of Cap/MCM-41 and Cap/TPA-MCM-41 were carried out under stirring as well as static conditions and results are shown in Figure 3. Under stirring condition, initially 44% Captopril was released and reached up to 98% in 26 h for Cap/MCM-41 while in case of Cap/TPA-MCM-41; initially 34% of drug was released and reached up to 89% in 30 h. For both systems, slower release of drug is observed, under static condition which may be due to the slower diffusion of drug molecules (Figure 3).

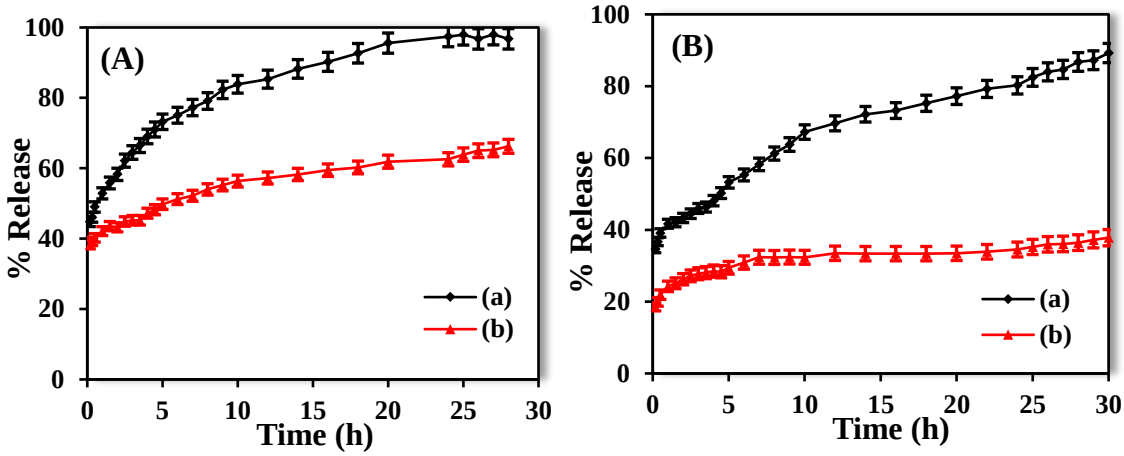

Figure 3. In vitro controlled release of (A) Cap/MCM-41 and (B) Cap/TPA-MCM-41 under (a) stirring and (b) static condition

(iii) Effect of pH on release rate of Captopril

To see the effect of pH on release rate of drug, in vitro release study of Captopril was carried out in different pH (1.2 and 7.4) and results are shown in Figure 4. At lower pH (SGF), higher release rate was observed for both systems (Cap/MCM-41 and Cap/TPA-MCM-41) as compared to higher pH (SBF) which may be because of the action of COOH group of Captopril. However, slower release was obtained for Cap/TPA-MCM-41 compared to Cap/MCM-41. Here also TPA plays major role in release rate of drug which is further explained in section (iv).

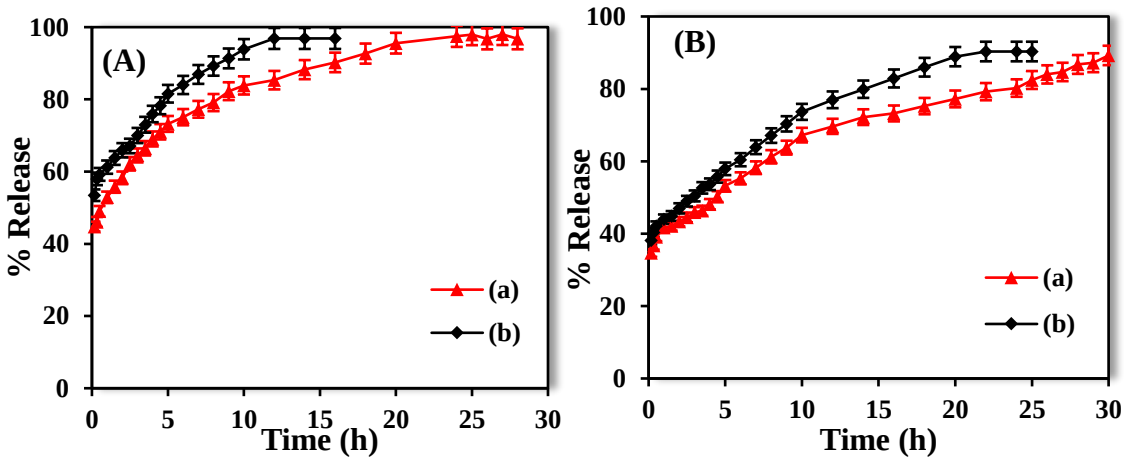

Figure 4. In vitro release of **(A)** Cap/MCM-41 and **(B)** Cap/TPA-MCM-41 at pH (a)7.4 (SBF) and (b) 1.2 (SGF)

(iv) Effect of TPA on release rate of Captopril

To investigate the action of TPA on release rate of drugs, release profile of drug loaded into pure materials were compared with functionalized materials and results are shown in Figure 5. Initially, 44% and 34% of Captopril was released and reached up to 83% and 67% in 10 h for MCM-41 and TPA-MCM-41, respectively. It reached up to 96% in 25 h and 87% in 29 h for MCM-41 and TPA-MCM-41, respectively. Here, more controlled release profile is obtained from TPA-MCM-41 as compared to pure MCM-41.

Burst release is observed for drugs which were loaded into pure MCM-41. This may be due the release of drug molecules which are present on the surface of carrier. However, more controlled release profile is obtained from TPA-MCM-41 as compared to pure MCM-41. This may be because better interactions between the drug molecules and TPA-MCM-41. As stated earlier, TPA has free terminal oxygen through which it can bind with drug. This may be the reasons of slower release of drugs from TPA-MCM-41.

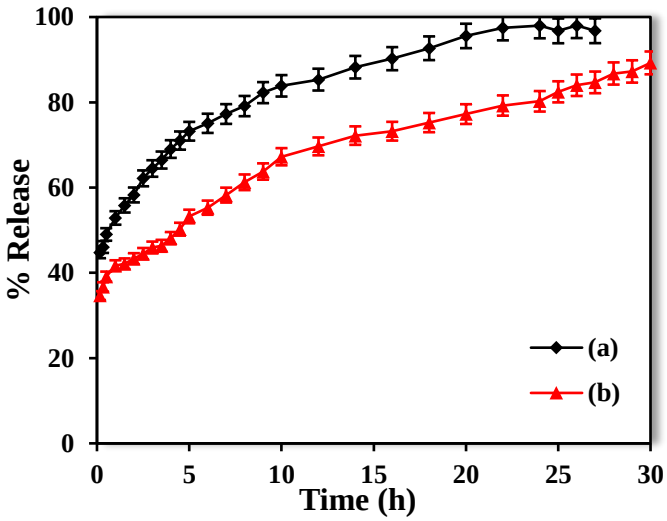

Figure 5. Comparison of in vitro release profile of (a) Cap/MCM-41 and (b) Cap/TPA-MCM-41

FTIR analysis of Cap/TPA-MCM-41 after release study was also carried out to confirm that TPA act as only functionalizing agent and its structure remain intact during release study and spectrum is shown in Figure 6. FTIR spectrum of Cap/TPA-MCM-41 is similar with that of TPA-MCM-41 (Figure 2b, Chapter 1b) which confirmed that structure of TPA remains intact in Asp/TPA-MCM-41 even after release study and it's truly act as functionalizing agent.

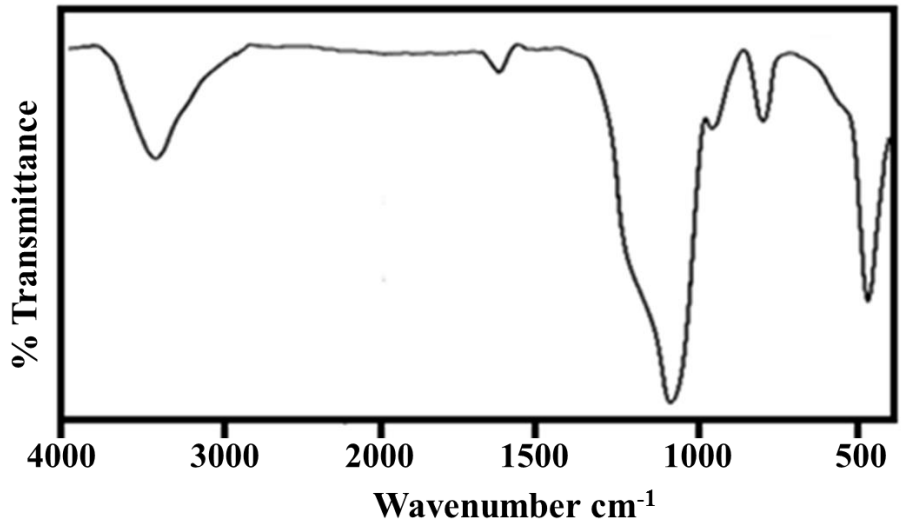

Figure 6. FTIR spectrum of Cap/TPA-MCM-41 after release study

Kinetic and Mechanism

To investigate drug release kinetic and mechanism, release data up to 10 h were fitted with First ordered release Kinetic Model and Higuchi Model.

(i) First ordered release kinetic model

Figure 7 shows plot of log of percentage remaining data against time and the kinetic parameters obtained are shown in Table 1. It was found that the release of Captopril follows the first order kinetic with linearity. Further, higher linearity and higher co-relation coefficient were obtained for Cap/TPA-MCM-41 (R^2= 0.9902) as compared to Cap/MCM-41 (0.9896).

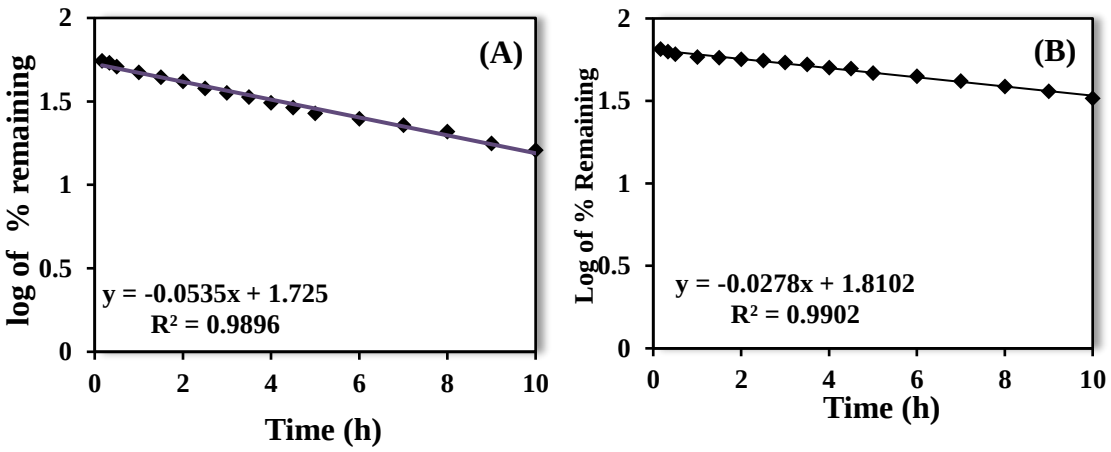

Figure 7. First order release kinetic model for (A) Cap/MCM-41 and (B) Cap/TPA-MCM-41

(ii) Higuchi Model

The release data were fitted to the Higuchi model and results are shown in Figure 8 and kinetic parameter in Table 1. The release mechanism of Captopril is best explained by this model with high linearity and high correlation coefficient (R^2) value for Cap/TPA-MCM-41 (R^2 = 0.9933) as compared to Cap/MCM-41 (R^2 = 9918). Higher value of R^2 suggests, more ordered release of Captopril from TPA-MCM-41 as compared to pure MCM-41. Thus kinetic and mechanistic studies show that drug release is concentration dependent process, follows first order release kinetics as well as the Fickian diffusion mechanism.

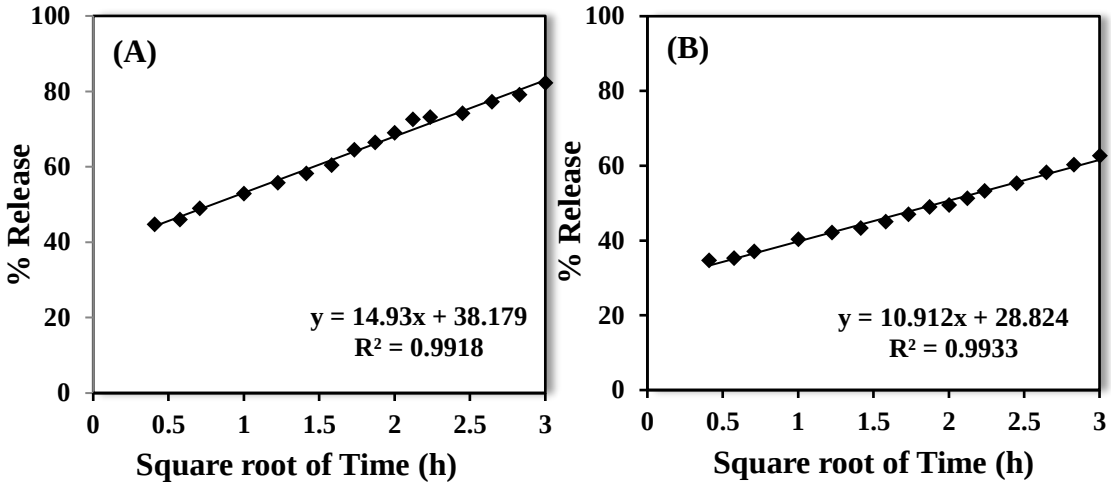

Figure 8. Higuchi Model for (A) Cap/MCM-41 and (B) Cap/TPA-MCM-41

Table 1. Kinetic parameters obtained from First order release kinetic model and Higuchi model

Model	Cap/MCM-41	Cap/TPA-MCM-41
First order release kinetic model	K_1 = 0.0535 R_1 = 0.986	K_1 = 0.0278 R_1 = 0.990
Higuchi model	K_2 = 14.93 R_2 = 0.991	K_2 = 10.91 R_2 = 0.993

In vitro controlled release of Aspirin

(a) Preparation of calibration curve for Aspirin

Stock solution of Aspirin was prepared by dissolving 10 mg in 100 ml SBF. From this stalk solution 20-200 ug/mL solutions were prepared by diluting specific amounts of stalk solution using SBF. The absorption of prepared solutions was taken at 296 nm wavelength using Perkin Elmer UV-Visible spectrophotometer. Using same method, working curve under SGF was also obtained and shown in Figure 9.

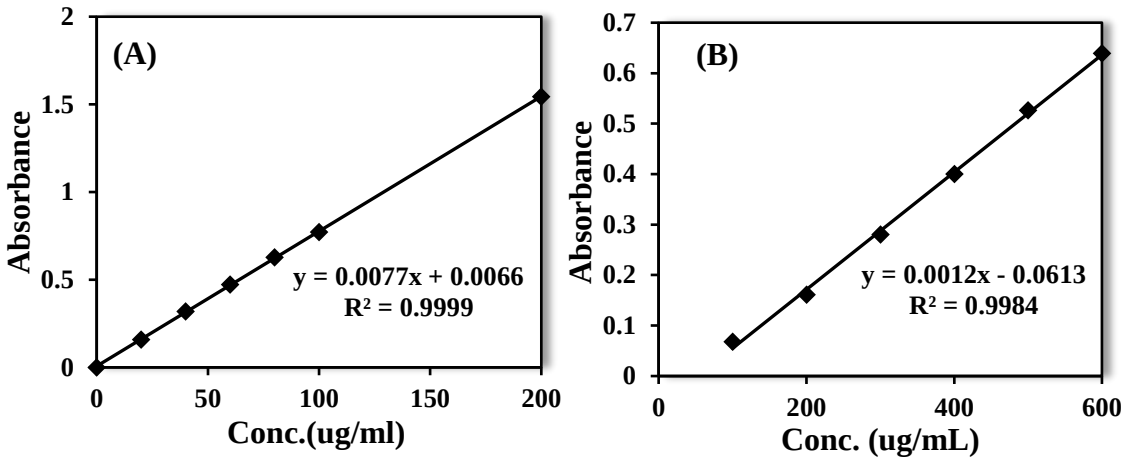

Figure 9. Calibration curve of Aspirin in (A) SBF (pH 7.4) and (B) SGF (pH 1.2)

(a) In vitro controlled release of Aspirin

In vitro release of Aspirin was carried out by soaking drug loaded samples in 100 mL SBF at 200 rpm at 37 ^{o}C temperature under. At predetermine time interval, 1 mL of release fluid was taken and fresh SBF was added to maintain the constant volume of the system. The 1 mL fraction was diluted and analyzed for Aspirin contain using UV-Visible spectrophotometry at 296 nm. Same release study in SGF (pH 1.2) was also carried out.

For finding out, whether the drug molecules are physically adsorbed or present inside the channels of the carrier, release study was carried out in SBF for physical mixture of drug (Aspirin) and carrier, prepared by mixing and grinding them physically.

Further, the release profile of Aspirin was compared with that of the marketed formulation of the drug, i.e., Ecosprin, which was obtained using the same method.

Result and discussion

(a) Comparison with physical mixture

In order to see whether the Aspirin molecule only physically adsorbed on the outer surface of material or not, release profile of Aspirin loaded material and physical mixture of Aspirin and carrier was compared and shown in Figure 10.

It is clear from the Figure 10 that physical mixture shows 100% dissolution of Aspirin within 1 h. while Aspirin loaded material shows controlled and ordered release which suggests the presence of Aspirin molecule inside the channel of carrier. This is already confirmed by BET surface area analysis.

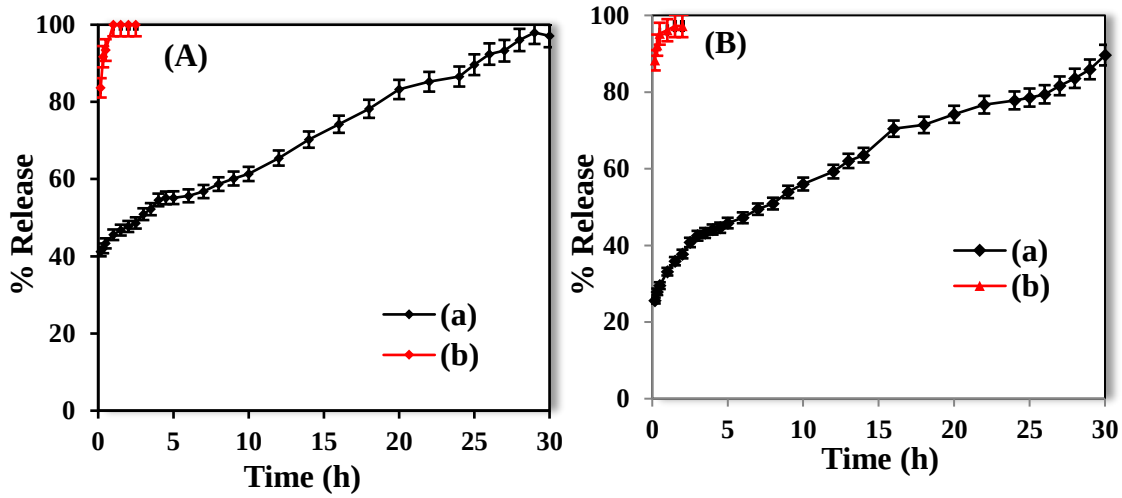

Figure 10. Comparison of release profile of (A) **a** Asp/MCM-41 and (B) **a** Asp/TPA-MCM-41 with **b** physical mixture

(b) Effect of stirring on release rate of drug

In order to see the effect of stirring on release rate of Aspirin, in vitro release study was carried out under two different conditions: (1) stirring as well as (2) static and results are shown in Figure 11. Under stirring condition, in case of Asp-MCM-41, initially 40% Aspirin was released and reached up to 99% in 30 h while in case of Asp/TPA-MCM-41 initially 25% of drug was released and reached up to 89% in 30 h. However, because of the slower diffusion of drug under static condition, slower release of Aspirin is observed for both systems.

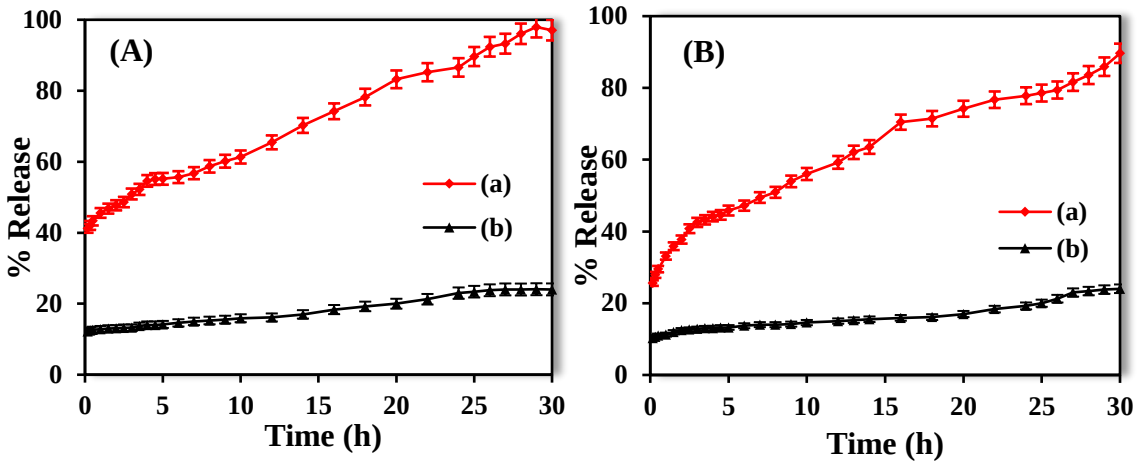

Figure 11. In vitro release of **(A)** Asp/MCM-41 and **(B)** Asp/TPA-MCM-41 under (a) stirring and (b) static conditions

(b) Effect of pH on release rate of drug

In order to see the effect of pH on release profile, release study was also carried out in simulated gastric fluid (SGF, pH 1.2) and compered with release profile obtained in simulated body fluid (SBF, pH 7.4) (Figure 12).

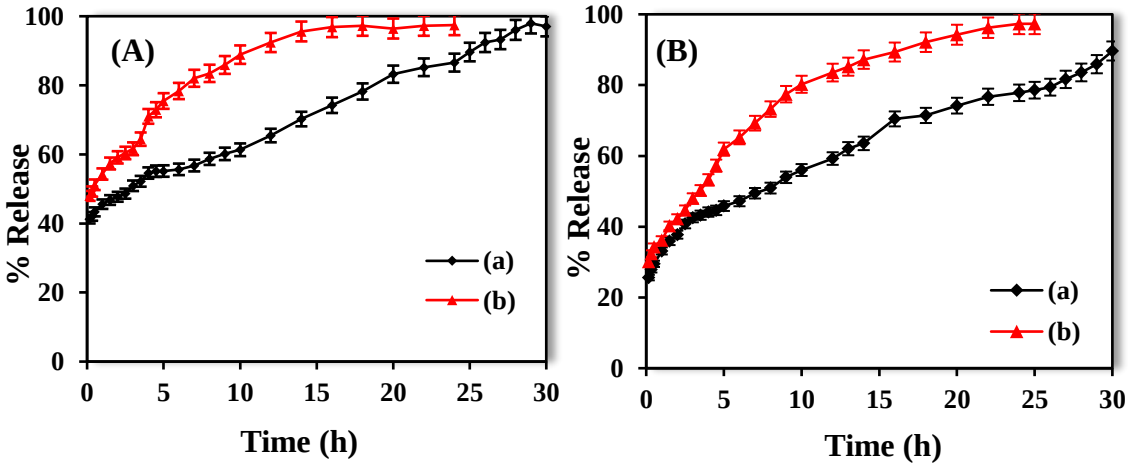

Figure 12. In vitro release of **(A)** Asp/MCM-41 and **(B)** Asp/TPA-MCM-41 at pH (a) 7.4 (SBF) and (b) 1.2 (SGF)

For both systems, Asp-MCM-41 and Asp/TPA-MCM-41, faster release of drug is observed at pH 1.2 compared to at pH 7.4. This is may be because protonation of COOH group of Aspirin occurred at pH 1.2 and hence C=O group is no longer present for hydrogen bonding with surface Si-OH group of materials. Thus, the interaction between drug and carrier become weak and hence faster release is observed under SGF.

(c) Effect of TPA on release rate of drug

To see the influence of TPA on release rate of Aspirin, release profile of Asp/MCM-41 and Asp/TPA-MCM-41 was compared and results are shown in Figure 13. Initially, 40% and 25% of Asp is released and reached up to 61% and 56% in 10 h for MCM-41 and TPA-MCM-41, respectively. It reached up to 98% and 89% in 30 h for MCM-41 and TPA-MCM-41, respectively. Here, more controlled release profile is obtained for Asp/TPA-MCM-41 as compared to Asp/MCM-41.

This is may be because of the more attractive interaction between the Aspirin molecules and TPA-MCM-41. As stated earlier, TPA has free terminal oxygens through which it can bind with drug. This may be the reasons of slower release of Aspirin from TPA-MCM-41.

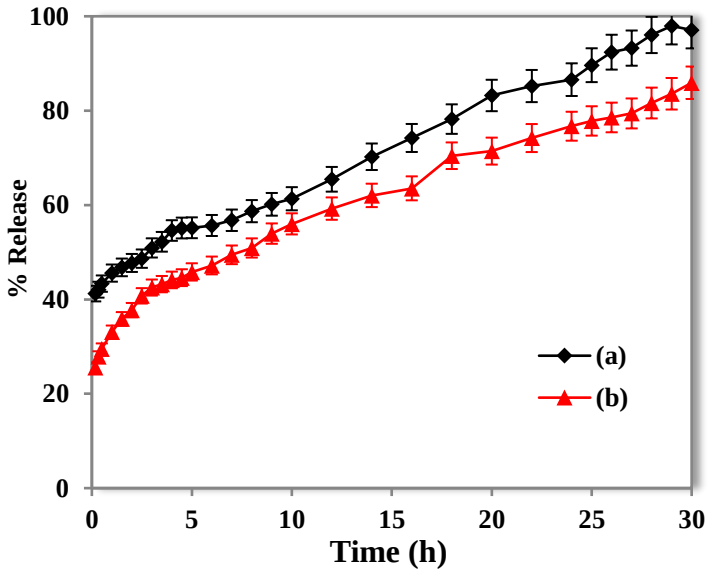

Figure 13. Comparison of Release profiles of Asp/MCM-41 and Asp/TPA-MCM-41

Further to confirm that TPA act as only functionalizing agent and its structure remain intact during release study, FTIR analysis of Asp/TPA-MCM-41 after release study was also carried out and spectrum is shown in Figure 14. FTIR spectrum of Asp/TPA-MCM-41 is similar with that of TPA-MCM-41 (Figure 2b) which confirmed that structure of TPA remains intact in Asp/TPA-MCM-41 even after release study and it's truly act as functionalizing agent.

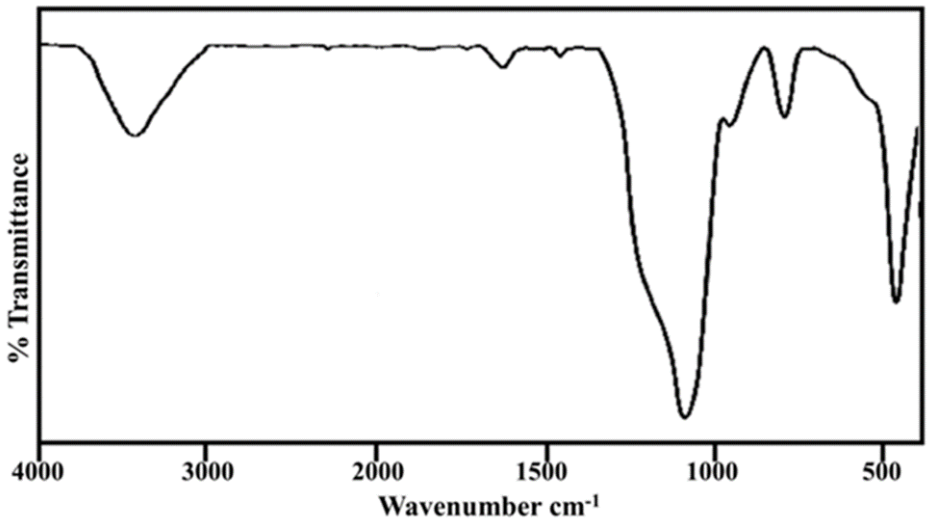

Figure 14. FTIR spectra of Asp/TPA-MCM-41 after release study

(d) Comparison of release profile of Asp/MCM-41, Asp/TPA-MCM-41 with marketed formulation (Ecosprin)

We have compared the release data of our formulation with conventional formulated drug and results are shown in Figure 15. Initially, 6% of Aspirin is released from conventional formulated drug (Ecosprin) and reached to 43% up to 1 h. However, 25% of drug is released from TPA-MCM-41 and reached to 33% up to 1 h. More delayed and ordered release profile is obtained for Asp/TPA-MCM-41 compared to Ecosprin.

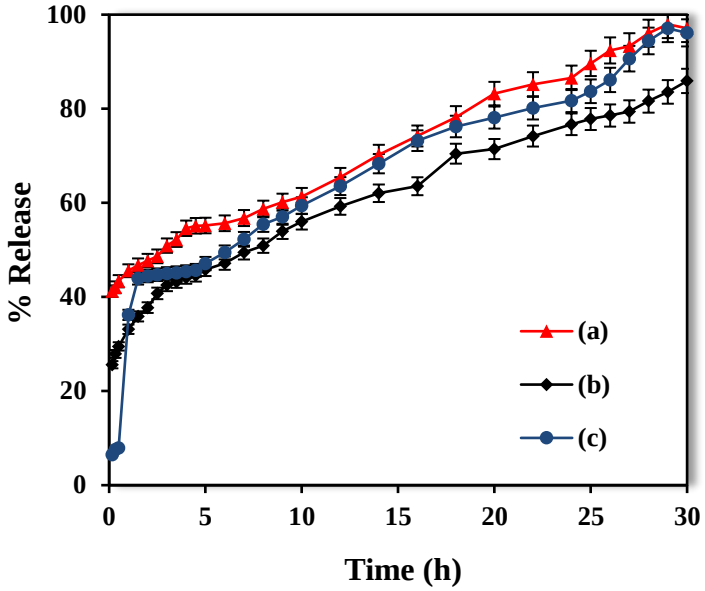

Figure 15. Comparison of release profiles of (a) Asp/MCM-41, (b) Asp/TPA-MCM-41 and (c) Ecosprin

Kinetics and Mechanism

To investigate drug release kinetic and mechanism, The Aspirin release data were fitted with First ordered release Kinetic Model, Higuchi Model [50-52]. The type of diffusion of Aspirin in support as well as the relation between the surface properties and release rate was studied by Korsmeyer-Peppas Model (KPM) and Extended Kinetic Model (EKM) [53, 54].

(i) First order release kinetic model

Figure 16 shows first ordered release kinetic model of Asp/MCM-41 and Asp/TPA-MCM-41, where log of % drug remaining is plotted against time in h. The First order release kinetic model was best fitted with higher linearity and higher co-relation coefficient (R^2= 0.96645) for Asp/TPA-MCM-41. This suggests the, Aspirin release is concentration dependent process and more ordered release is obtained for Asp/TPA-MCM-41 system.

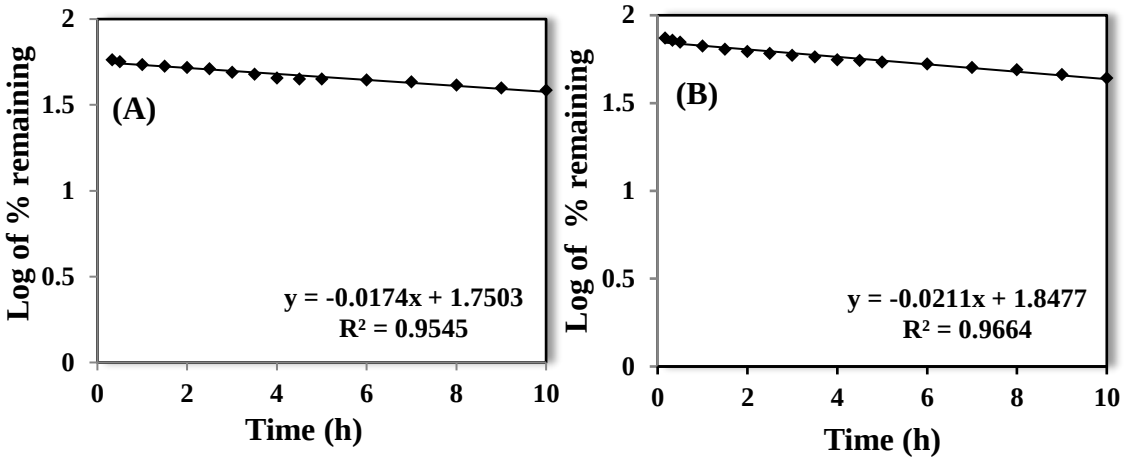

Figure 16. First order release kinetic model of **(A)** Asp/MCM-41 and **(B)** Asp/TPA-MCM-41

(ii) **Higuchi model**

The Higuchi model (Figure 17) describes the percentage release versus square root of time dependent process based on Fickian diffusion. According to this model release mechanism of drug involves simultaneous penetration of SBF into the pores, dissolution of drug molecule and diffusion of these molecules from the pores.

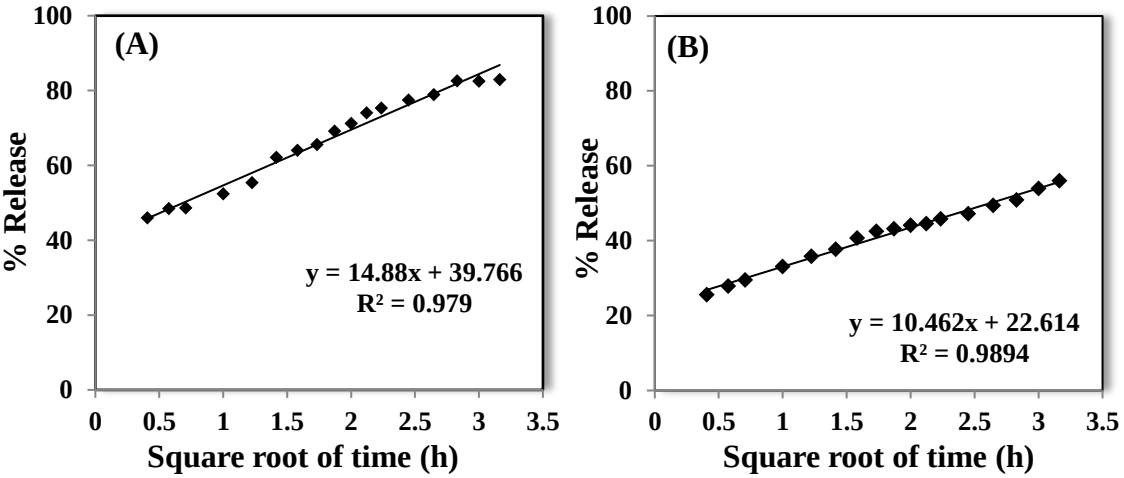

Figure 17. Higuchi Model of **(A)** Asp/MCM-41 and **(B)** Asp/TPA-MCM-41

The release mechanism of Aspirin is best explained by this model with high linearity and high correlation coefficient (R^2 = 0.9894) for Asp/TPA-MCM-41. This suggests that release of Aspirin follows Fickian diffusion mechanism as well as more ordered release profile was obtained in case of Asp/TPA-MCM-41.

(iii) Korsmeyer-Peppas Model

Korsmeyer and Peppas (1984) developed an empirical equation to analyze both Fickian and non-Fickian release of drug. $Mt/M\infty = Kt^n$. where, n is the empiric exponent which indicates type of release mechanism, i.e., n = 0, 1.0 and 0.5 indicates Zero-Order, First-order and Higuchi model respectively [55]. In the present case, the found value of n is 0.47 and 0.49 for Asp/MCM-41 and Asp/TPA-MCM-41 respectively, confirming that the present systems follow Higuchi model. For KPM, higher linearity and correlation Co-efficient (R^2) was obtained for Asp/TPA-MCM-41 (Figure 18).

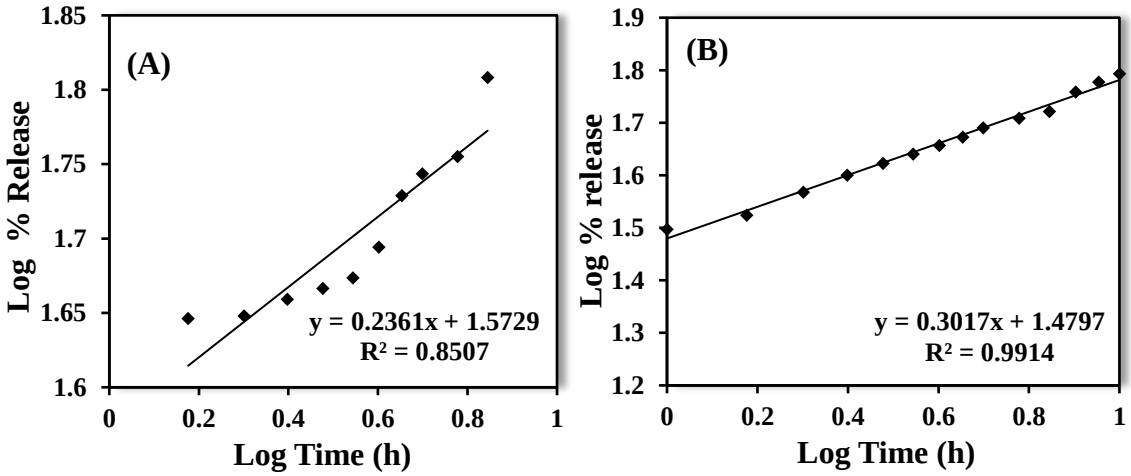

Figure 18. KPM for **(A)** Asp/MCM-41 and **(B)** Asp/TPA-MCM-41

(iv) Extended Kinetic Model

EKM model describes the drug concentration dynamics in the bulk liquid, on solid and at the interface. It includes the diffusion steps for the drug transport in pores and in the external liquid film (surrounding the carrier) to the bulk liquid. Due to the concentration gradients, the drug follows diffusion path in the pores and external liquid film. The estimated kinetic parameters of EKM model are shown in Table 2 and EKM prediction of the drug concentration dynamics in the bulk liquid, on solid and at the interface are displayed in Figure 19 for Asp/MCM-41 and Asp/TPA-MCM-41. On comparing the estimated desorption-adsorption equilibrium constants $K = k_2/k_1$ from Table 2, it is clear that release tendency is higher for Asp/MCM-41 (K = 5.60) compared to Asp/TPA-MCM-41 (K = 4.59) and hence controlled release profile was obtained for latter case. This may be because of the interaction of Aspirin with TPA, which can control the rate of release for longer time.

Concentration dynamics

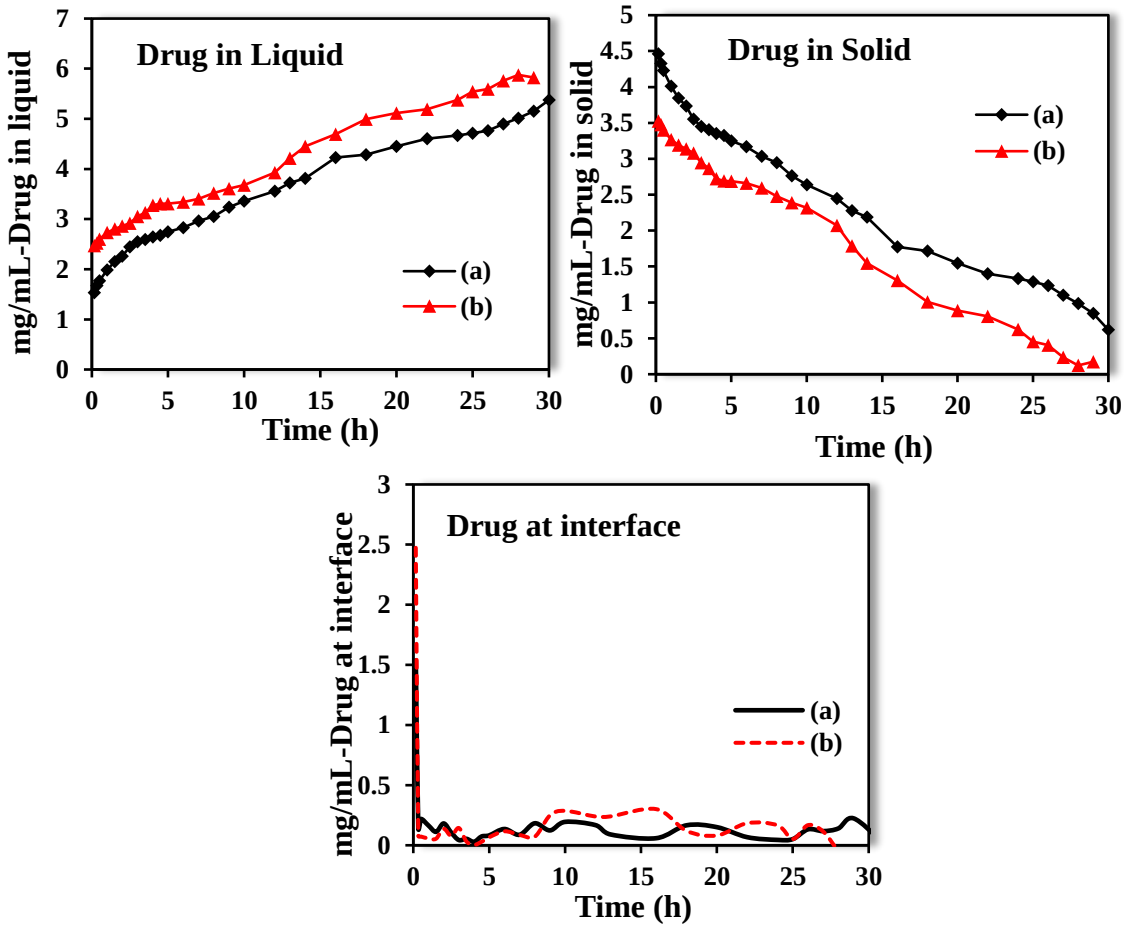

Figure 19. Experimental data and predictions of Asp release from **(a)** TPA-MCM-41 and **(b)** MCM-41 in SBF by Extended Kinetic Model

Table 2. Estimated parameters of KPM and EKM model for Asp release from MCM-41 and TPA-MCM-41. Units: k_1, k_2 (h^{-1} mL mg^{-1}); K= k_2/k_1

Materials	Model			
	First order release kinetic Model	Higuchi Model	Korsmeyer-Peppas Model	Extended Kinetic Model
Asp/MCM-41	K_1= 0.0174 R_1=0.954	K_2= 14.88 R_2= 0.979	k_1= 0.0166 K= 5.60	n = 0.47
Asp/TPA-MCM-41	K_1= 0.0211 R_1= 0.966	K_2= 10.462 R_2= 0.989	k_1= 0.0103 K= 4.59	n = 0.49

In vitro controlled release of Camptothecin

Preparation of calibration curve for Camptothecin

Stock solution of Camptothecin (CPT) was prepared by dissolving 10 mg in 100 ml SBF. From this stalk solution 2-18 ug/mL solution were prepared by diluting specific quantities of stalk solution using SBF. The absorption of prepared solutions was taken at 370 nm wavelength using Perkin Elmer UV-Visible spectrophotometer and calibration curve is shown in Figure 20A. Using same method calibration curve was also obtained in SGF (Figure 20B).

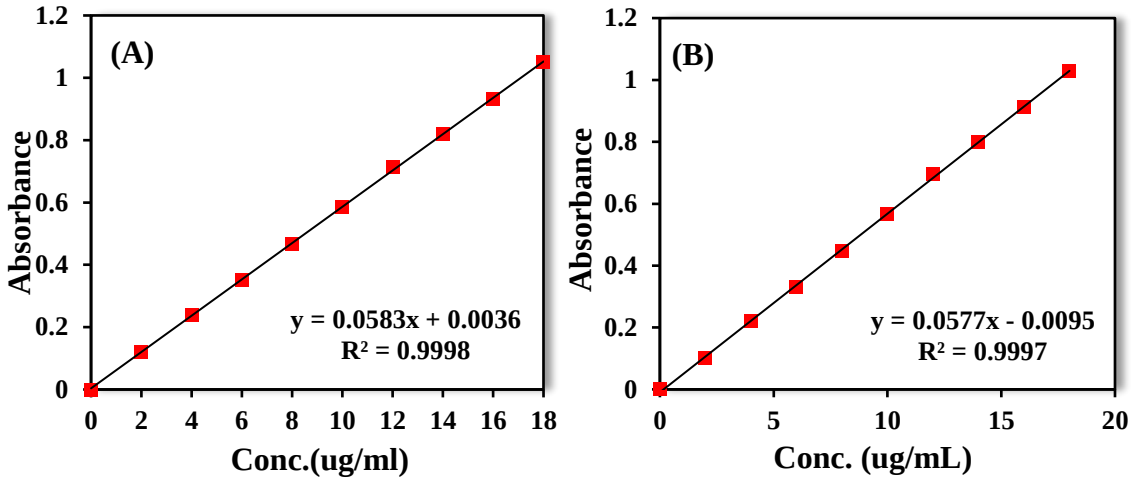

Figure 20. Calibration curve of Camptothecin in (A) SBF and (B) SGF

(a) In vitro controlled release of Camptothecin

In vitro release of CPT was carried out by soaking drug loaded samples in 100 mL of SBF at 200 rpm at 37 ^{o}C temperature. At proper time interval, 1 mL of release fluid was taken and fresh SBF was added to maintain the constant volume of the system. The 1 mL fraction was diluted and analyzed for CPT contains using UV-Visible spectrophotometry at 370 nm.

Results and Discussion

(a) Comparison with physical mixture

Release profile of CPT was also compared with its physical mixture (CPT + carrier) and shown in Figure 21. It is clear from the Figure 20 that physical mixture shows 100% dissolution of CPT within 1 h. while CPT loaded material shows controlled and ordered release which suggests the presence of CPT molecule inside the channel of carrier. This is already confirmed by BET surface area analysis.

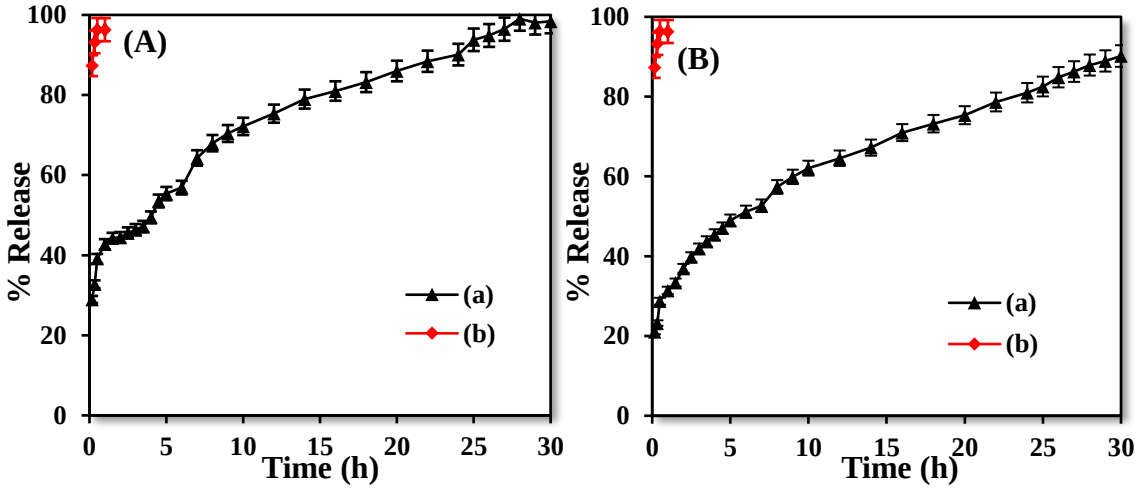

Figure 21. Comparison of release profile of (A) **a** CPT/MCM-41 and (B) **a** CPT/TPA-MCM-41 with **b** physical mixture

(b) Effect of Stirring on release rate of drug

To evaluate the effect of stirring on release rate of CPT, release study was carried out under stirring and static condition and results are shown in Figure 22. It is observed that under static condition slower release profile is obtained for both systems i.e CPT/MCM-41 and CPT/TPA-MCM-41. Under static condition, initially, 18% and 10% of CPT was release which reached up to 33% and 27% in 10h for MCM-41 and TPA-MCM-41, respectively. However, comparatively fast release profile is obtained under stirring condition for both systems. Slower diffusion of CPT molecules, under static condition could be the Reason of slower release of CPT.

To see the effect of pH on release rate, release study was also carried out in SGF which is similar to that of result which was obtained in SBF.

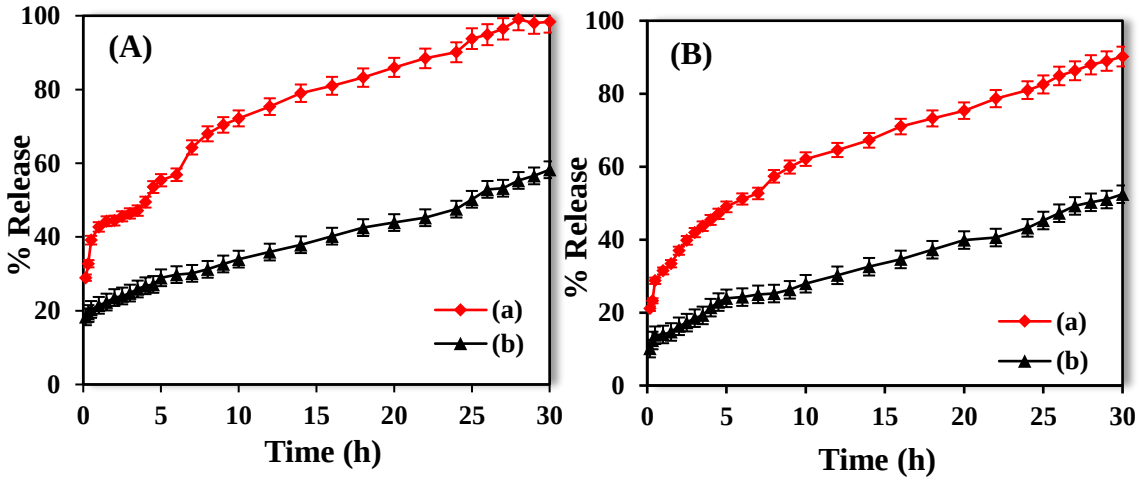

Figure 22. In vitro release profile of CPT/MCM-41 and CPT/TPA-MCM-41 under (a) stirring and (b) static condition

(a) Effect of TPA on release rate

To see the influence of TPA on release rate of CPT, release profile of CPT/MCM-41 and CPT/TPA-MCM-41 was compared and results are shown in Figure 23. Initially, 28% and 21% of CPT was released and reached up to 72% and 62% in 10 h from MCM-41 and TPA-MCM-41, respectively. It reached up to 98% and 90% in 30 h for MCM-41 and TPA-MCM-41, respectively. Here, slower release profile is obtained for CPT/TPA-MCM-41 as compared to CPT/MCM-41. This is may be because of the more attractive interaction between the CPT molecules and TPA-MCM-41. As stated earlier, TPA has terminal free oxygen through which it can bind with drug. This is may be the reasons of slower release of CPT from TPA-MCM-41.

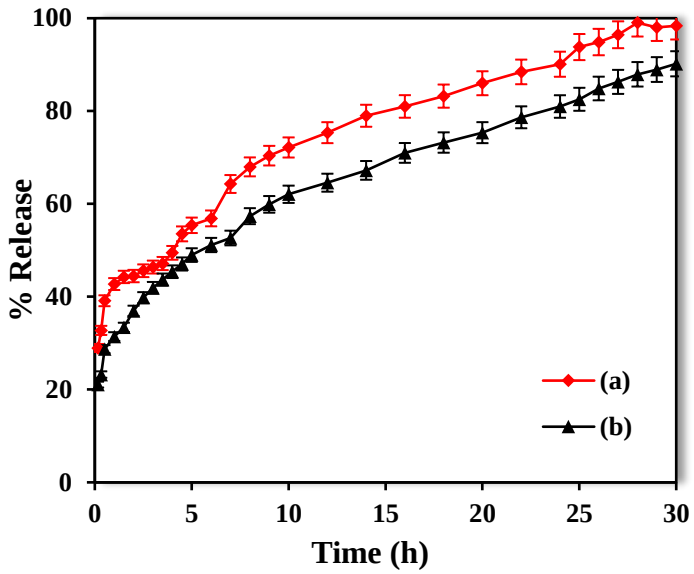

Figure 23. Comparison of Release profile of CPT/MCM-41 and CPT/TPA-MCM-41

Kinetics and Mechanism

To investigate drug release kinetic and mechanism, the CPT release data were fitted with First ordered release Kinetic Model, Higuchi Model. The type of diffusion of CPT in support as well as the relation between the surface properties and release rate was studied by Korsmeyer-Peppas Model (KPM) and Extended Kinetic Model (EKM).

(i) First order release kinetic model

First order release kinetic model is used to study the dissolution of drug encapsulated in porous matrices. According to this model, rate of release is concentration dependent. Figure 24 shows first ordered release kinetic model of CPT/MCM-41 and CPT/TPA-MCM-41, where log of % remaining data are plotted against time in h and kinetic parameters are shown in Table 3. The First order release kinetic model was best fitted with higher linearity and higher co-relation coefficient (R^2= 0.9775) for CPT/TPA-MCM-41. This suggests the, CPT release is concentration dependent process and more ordered release is obtained for CPT/TPA-MCM-41 system.

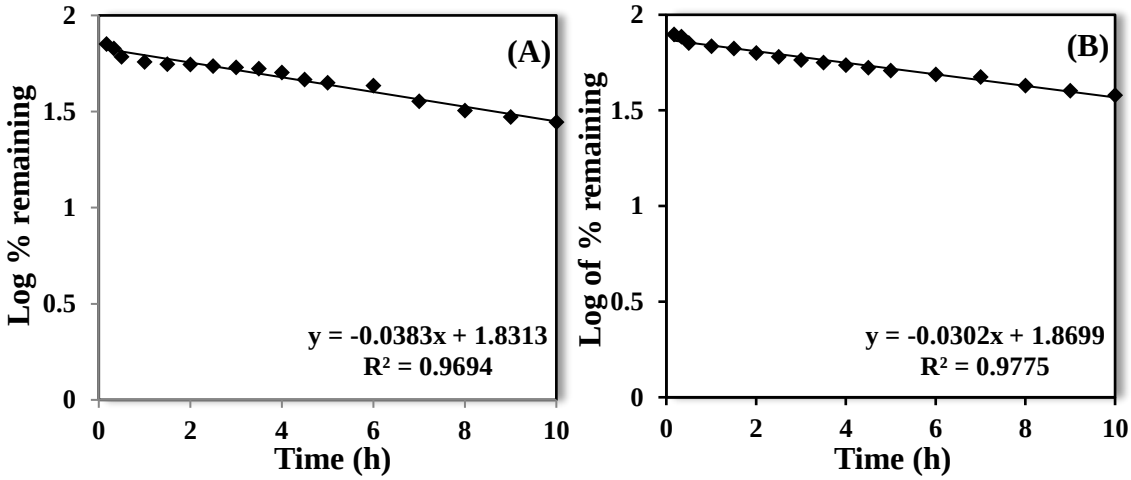

Figure 24. First order release kinetic model of (A) CPT/MCM-41 and (B) CPT/TPA-MCM-41

(ii) Higuchi model

The Higuchi model (Figure 25) describes the percentage release versus square root of time dependent process based on Fickian diffusion. According to this model release mechanism of drug involves simultaneous penetration of SBF into the pores, dissolution of drug molecule and diffusion of these molecules from the pores. The release mechanism of CPT is best explained by this model with high linearity and high correlation coefficient (R^2 = 0.997) for CPT/TPA-MCM-41. This suggests that release of CPT follows Fickian diffusion mechanism as well as more ordered release profile was obtained in case of CPT/TPA-MCM-41.

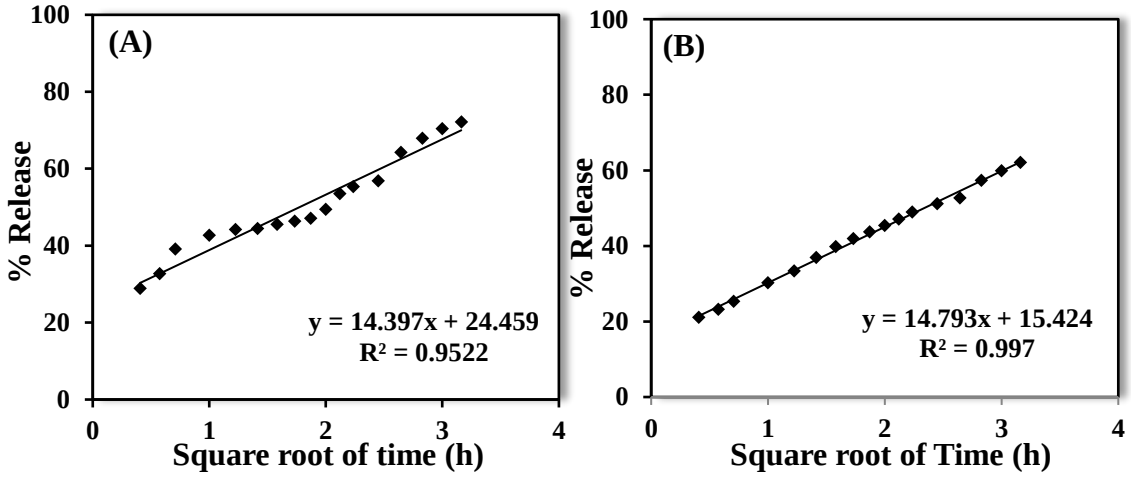

Figure 25. Higuchi model of (A) CPT/MCM-41 and (B) CPT/TPA-MCM-41

(iii) Korsmeyer-Peppas Model

In the present case, the found value of n is 0.48 and 0.5 for CPT/MCM-41 and CPT/TPA-MCM-41 respectively (Figure 26), confirming that the present systems follow Higuchi model. For KPM, higher linearity and correlation Co-efficient (R^2) was obtained for CPT/TPA-MCM-41.

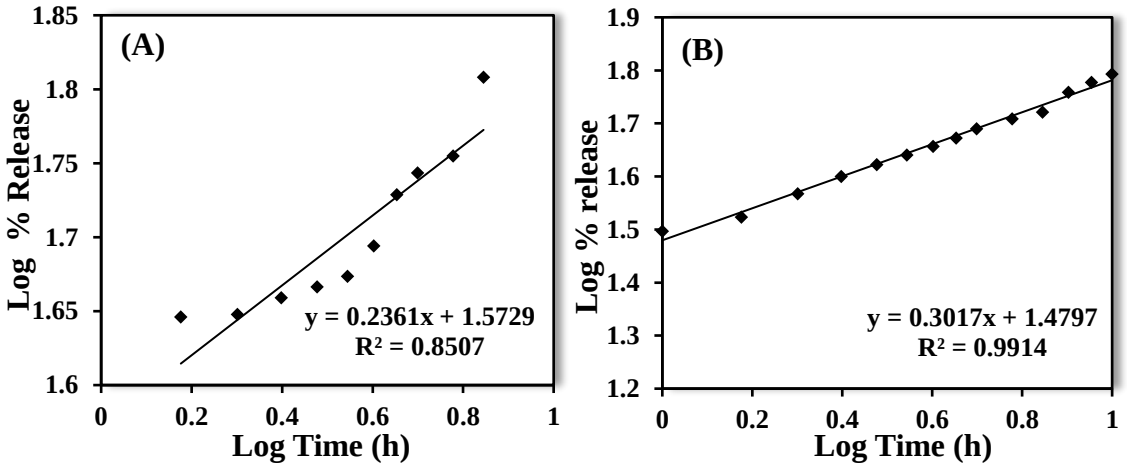

Figure 26. KPM model for (A) CPT/MCM-41 and (B) CPT/TPA-MCM-41

(iv) Extended Kinetic Model

The estimated kinetic parameters of EKM are shown in Table 2 and EKM prediction of the drug concentration dynamics in the bulk liquid, on solid and at the interface are displayed in Figure 27 for CPT/MCM-41 and CPT/TPA-MCM-41. On comparing the estimated desorption-adsorption equilibrium constants $K = k_2/k_1$ from Table 2, it is clear that release tendency is higher for CPT/MCM-41 (K =6.19) compared to CPT/TPA-MCM-41 (K = 4.76). This may be due to the strong interaction of CPT with terminal oxygen of TPA which can hold the CPT molecules for longer time.

Concentration dynamics

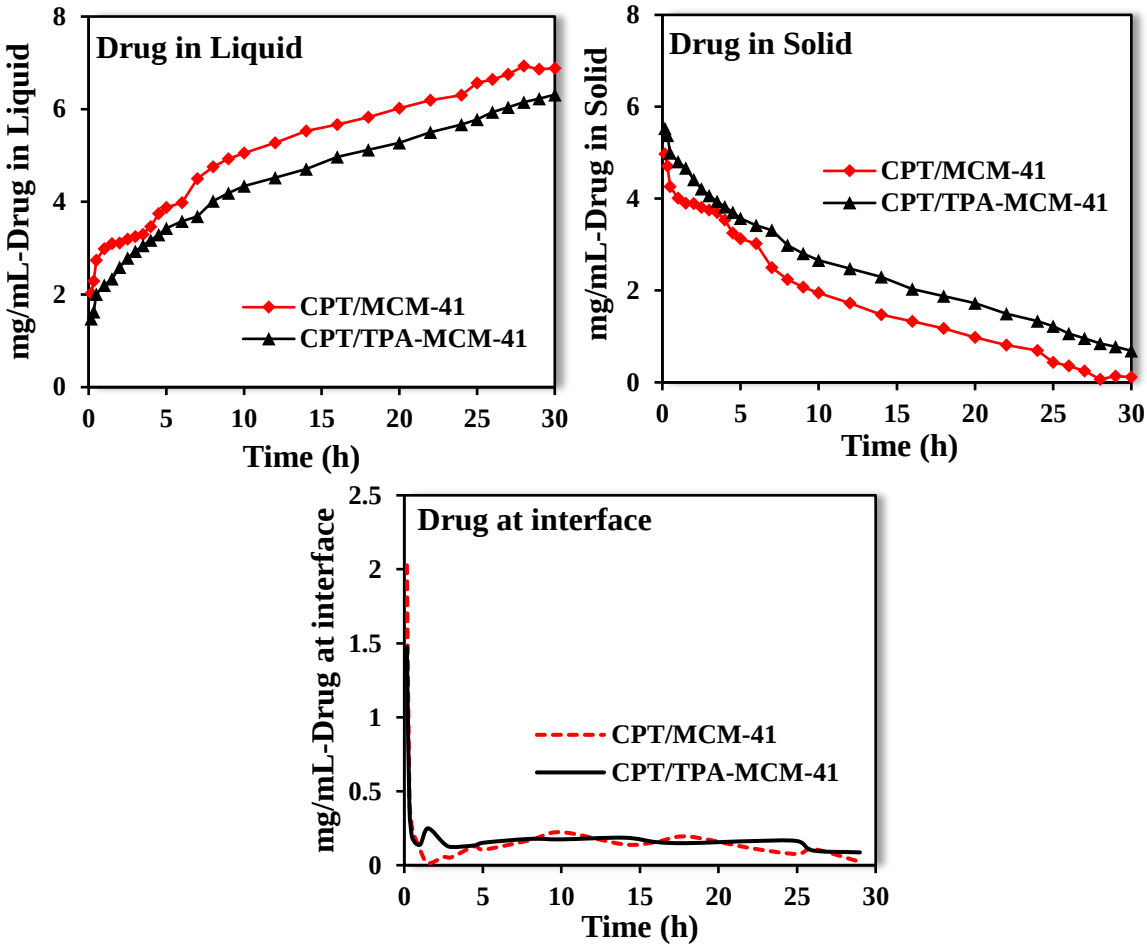

Figure 27. Experimental data and predictions of CPT release from MCM-41 and TPA-MCM-41 in SBF by Extended Kinetic Model

Table 2. Estimated parameters of KPM and EKM model for CPT release from MCM-41 and TPA-MCM-41. Units: k_1, k_2 (h^{-1} mL mg^{-1}); $K = k_2/k_1$

Materials	Model			
	First order release kinetic Model	Higuchi Model	Extended EKM:	Korsmeyer-peppas KPM:
CPT/MCM-41	K_1= 0.0383 R_1=0.9694	K_2= 14.397 R_2= 0.9522	k_1= 0.0061 K= 6.19	n = 0.48
CPT/TPA-MCM-41	K_1= 0.0302 R_1= 0.9775	K_2= 14.793 R_2= 0.997	k_1= 0.0105 K= 4.76	n = 0.5

Cytotoxicity study

(i) In Vitro Study:

Human hepatocellular liver carcinoma (HepG2) cells were incubated at 37 °C with 5% CO_2 in a water jacketed CO_2 incubator (Thermo Scientific, Forma series II 3111, USA). Cells were seeded (1×10^5 cells) in a T25 flask and cultured in DMEM (Dulbecco's Modified Eagle Medium, High Glucose) containing 10% Fetal bovine serine (FBS) and 1% antibiotic-antimitotic solution. Cells were trypsinized every third day by sub culturing with TPVG (Trypsin Phosphate Versene Glucose) solution.

(ii) Cytotoxicity Assay:

Cytotoxicity was determined by 3-(4, 5-dimethylthiazol-2-yl)-2,5-diphenyltetrazolium bromide (MTT) assay. Cells (7×10^3 cells/well) were seeded in 96-well culture plates for 24 h and then treated with 0.1, 0.3 and 0.5 mg/mL concentrations of MCM-41, TPA-MCM-41, CPT/TPA-MCM-41 for 24 h. The doses of CPT treatment were 5, 15 and 25 μg/mL that were proportionate to the amount of CPT released from 0.1, 0.3 and 0.5 mg/mL CPT/TPA-MCM-41 respectively. Later on, 10 μL of MTT (5 mg/mL) was added followed by incubation for 4 h at 37 °C. Formazan formed at the end of the reaction was dissolved in 150 μL of DMSO and absorbance was read at 540 nm using an ELX800 Universal Microplate Reader (Bio-Tek instruments, Inc., Winooski, VT) and the percentage cytotoxicity was calculated [56].

Evaluation of in vitro cytotoxicity-MTT assay

Induction of apoptosis in cancer cells leading to their termination has been extensively reported by use of several anti-cancer agents including Camptothecin (CPT). Inhibition of topoisomerase followed by cytochrome C release and mitochondrial hyperpolarization is reported to be induced by CPT in mammalian cancer cells [33]. Mitochondrial dysfunction is assessed by MTT assay to establish anticancer potential of test compounds. In the present study, Human hepatocellular liver carcinoma (HepG2) cells were treated with MCM-41, TPA-MCM-41, CPT/TPA-MCM-41 or CPT and MTT assay was performed. Metabolically active cells produce a purple coloured formazan at the end of the assay and the intensity of colour reflects upon the functional status of mitochondria [56, 57]. MCM-41 showed ≤ 10% cytotoxicity in the said doses

(0.1, 0.3, 0.5 mg/ml, Figure 28). The functionalized material, TPA-MCM-41 recorded < 30% cytotoxicity whereas functionalized carrier loaded with drug CPT (CPT/TPA-MCM-41) showed > 40% at 0.5 mg/ml dose. These observations are of relevance because CPT/TPA-MCM-41 (at 0.5 mg/ml where in 25µg/mL CPT was released) accounted for 9.2% higher cytotoxicity than CPT treated group at the same dose. Overall, the results indicate that the TPA-MCM-41 carrier is non-toxic to the cells but the drug loaded carrier accounts for highest percentage of cytotoxicity amongst all groups. These results imply towards CPT/TPA-MCM-41 mediated improved delivery of CPT that can be of significance in cancer therapy.

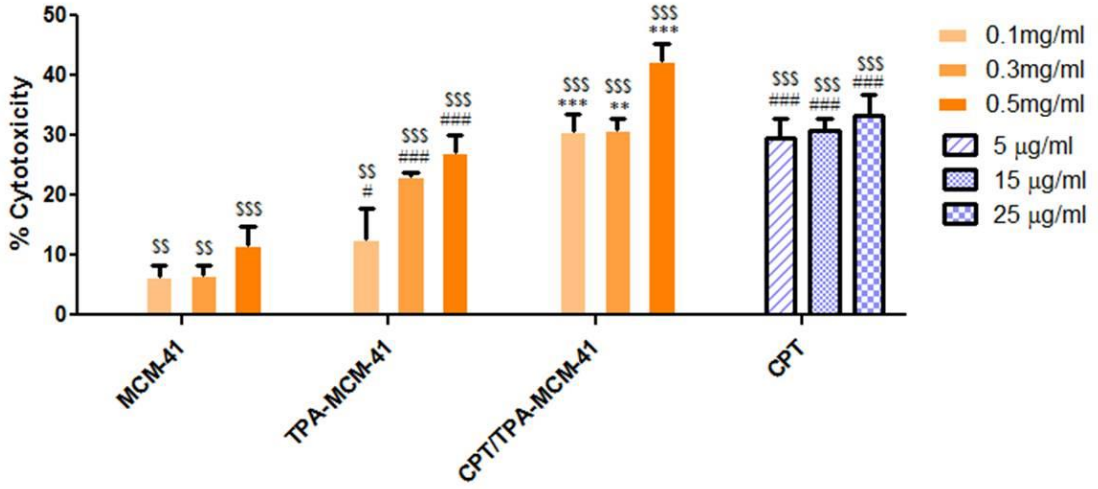

Figure 28. Effect of materials on the cytotoxicity of HepG2 cells. Control cells did not show cytotoxicity. Results are expressed as mean ± SD for n=3. $$P < 0.01 and $$$P < 0.001 as compared to control of respective groups and #P < 0.05, ###P < 0.001 as compared to respective concentrations of MCM-41. **P < 0.01 and ***P < 0.001 as compared to respective concentrations of TPA-MCM-41.

Conclusions

- In vitro release study of shows that stirring has great influence on release rate of all the drugs. Under static condition, slower release was observed for all the drugs, as in this condition diffusion of molecules became slower.
- In vitro release study under different acidic pH shows that release rate of Captopril as well as Aspirin has become faster at lower pH. At lower pH, C=O group of drug became protonated and hence interaction between drug and carrier decreases. However, pH does not show any effect on release rate of Camptothecin.
- Further, comparison of release profile of drug loaded materials and physical mixture (drug + carrier) shows that drug molecules are truly present inside the channels of carrier and not on the surface.
- It also shows that TPA has tremendous effect on release rate of all the drugs. As having number of terminal oxygen through which it binds with drugs and hold them for longer time. Hence, slower and ordered release was obtained for Cap/TPA-MCM-41, Asp/TPA-MCM-41 and CPT/TPA-MCM-41 systems.
- FTIR after release study of Cap/TPA-MCM-41, Asp/TPA-MCM-41 and CPT/TPA-MCM-41 shows that TPA remains intact even after release and hence prove that TPA acts truly as functionalizing agent.
- Kinetic and mechanistic study shows that release of Captopril follows first ordered release kinetic model and Higuchi diffusion mechanism. Release of Aspirin as well as Camptothecin also follows the same mechanism which was further supported by Korsmeyer Peppas Model and Extended kinetic Model.
- For behaving as true carrier, material should be non-cytotoxic. For finding this, MTT study of MCM-41, TPA-MCM-41, CPT/TPA-MCM-41 and pure CPT has also been carried out which suggests that all materials are non-cytotoxic accept one which are drug loaded.

References

[1] T. Takagi, C. Ramachandran, M. Bermejo Y. Yu SLX, G.L. Amidon, 2006. Mol. Pharm. 3, 6, 631 (2006).

[2] D.W. Cushman, M.A. Ondetti,s Hypertension 17,589 (1991).

[3] H.F. Askal, 1991. Talanta. 38, 10, 1155 (1991)

[4] Qu. Fengyu, Zhu. Guangshan, H. Shiying S. Li, J. Sun, D. Zhang, S. Qiu, Microporous Mesoporous Mater. 92, 1 (2006).

[5] A.O. Nur, J.S. Zhang, Int. J. Pharmaceut. 66, 139 (2000).

[6] F. Qu, G. Zhu, S. Huang, S. Li, J. Sun, D. Zhang, S. Qiu, Microporous Mesoporous Mater. 92, 1 (2006).

[7] R. F. Popovici, C.T. mihai, E.M. Seftel, P. Rotinberg, E. Popovici, V.A. Voicu, J. Nanomater. Biostruct. 6, 999, (2011).

[8] F. Qu, G. Zhu, S. Huang, S. Li, S. Qiu, Chem. Phys. Chem. 7, 400 (2006).

[9] R.F. Popovici, E.M. Seftel, G.D. Mihai, E. Popovici, V.A. Voicu, J. Pharma. Sci. 100, 704 (2011).

[10] S.D. Talekar, R.V. Haware, R.H. Dave, Eur. J. Pharm. Sci. 15, 130, 215 (2019).

[11] F. Catella-Lawson, M.P. Reilly, S.C. Kapoor, A.J. Cucchiara, S. DeMarco, B. Tournier, S.N. Vyas, G.A. FitzGerald, New Eng. J. Med. 345, 1809 (2001).

[12] P.M. Ridker, N.R. Cook, I.M. Lee, D. Gordon, J.M. Gaziano, J.E. Manson, C.H. Hennekens, J.E. Buring, New Eng. J. Med. 352, 1293 (2005).

[13] X.L. Tan, K.M. Reid Lombardo, W.R. Bamlet, A.L. Oberg, D.P. Robinson, K.E. Anderson, G.M. Petersen, Cancer Prev. Res., 4, 1835 (2011).

[14] F. Catella-Lawson, M.P. Reilly, S.C. Kapoor, A.J. Cucchiara, S. DeMarco, B. Tournier, S.N. Vyas, G.A. FitzGerald, New Engl. J. Med. 2001, 345, 1809 (2001).

[15] S. Dreve, I. Kacso, A. Popa, O. Raita, F. Dragan, A. Bende, G. Borodi, I. Bratu, J. Mol. Struct. 997, 78 (2011).

[16] Z. Wei, X-F. Qian, Y-B. Zhang, J. Yin, Zi-K. Zhu, Mater. Res. Bull. 40, 766 (2005).

[17] G. Lin, J. Sun, Y. Li, J. Solid State Chem. 184, 1909 (2011).

[18] A. Datt, Izz El-Maazawi, S.C. Larsen, J. Phys. Chem. C 116, 18358 (2012)

[19] A. Datt, D. Fields, S.C. Larsen, J. Phys. Chem. C 116, 21382 (2012).

[20] X. Xu, Z. Gu, X. Chen, C. Shi, C. Liu, M. Liu, L.Wang, M. Sun, K. Zhang, Q. Liu, Y. Shen, C. Lin, B. Yang, H. Sun, Acta. Biomater. 1, 86, 235 (2019).

[21] F. Kavousi, M. Goodarzi, D. Ghanbari, K. Hedayati, J. Mole. Stru. 1183, 324 (2019).

[22] S. Farias, J.S. Boateng, Int. J. Pharm. 20, 553 (1-2) 65 (2018).

[23] M. Pishnamazi, J. Iqbal, S. Shirazian, G.M. Walker, M.N. Collins, Int. J. Biological Macromole. 124, 354 (2019).

[24] C.L. Peng, P.S. Lai, F.H. Lin, Yueh-Hsiu Wu S, M.J. Shieh, Biomaterials 30, 21, 3614 (2009).

[25] J.A. Gottlieb, A.M. Guarino, J.B. Call, V.T. Oliverio, J.B. Block, Cancer Chemother. Rep. 54, 461 (1970).

[26] F.M. Muggia, P.J. Creaven, H.H. Hansen, M.H. Cohen, O.S. Selawry, Cancer Chemother. Rep. 156, 515 (1972).

[27] C.G. Moertel, A.J. Schutt, R.J. Reitemeier, R.G. Hahn, Cancer Chemother. Rep. 156, 95 (1972).

[28] A. Shenderova, T.G. Burke, S.P. Schwendeman, Pharm. Res. 14, 1406 (1997).

[29] S.C. Yang, L.F. Lu, Y. Cai, J.B. Zhu, B.W. Liang, C.Z. Yang, J. Control. Release, 59, 299 (1999).

[30] B.B. Lundberg, Anticancer Drug Des. 13, 453 (1998).

[31] R. Cortesi, E. Esposito, A. Maietti, E. Menegatti, C. Nastruzzi, Int. J. Pharm. 159, 95 (1997).

[32] P. Botella, I. Abasolo, Y. Fernández, C. Muniesa, S. Miranda, M. Quesada, J. Ruiz, S. Schwartz Jr., A. Corma, J Control. Rel. 156, 246 (2011).

[33] M. Manikandan, K. Kannan, Asian. J. Pharm. Clin. Res, 9, 3, 71 (2016).

[34] Z-Y. Li, Y. Liu, X-Q. Wang, L-H. Liu, J-J. Hu, G-F. Luo, W-H. Chen, L. Rong, X-Z. Zhang, ACS Appl. Mater. Interfaces, 5, 7995 (2013).

[35] Z. Zhang, D. Balogh, F. Wang, S.Y. Sung, R. Nechushtai, I. Willne, ACS Nano. 7, 10, 8455 (2013).

[36] H. Wang, M. Dong, S. Khan, Su. Lu, R. Li, Y. Song, Y-N. Lin, N. Kang, C.H. Komatsu, M. Elsabahy, K.L. Wooley, ACS Macro. Lett. 7, 783 (2018).

[37] R. Rashmi, D. Nedungadi, A. Podder, N. Mishra, S. Bhuniya, J. Photochem. Photobiol. B. 189, 14 (2018).

[38] A. Plichta, S. Kowalczyk, E. Olędzka, M. Sobczak, M. Strawski, Int. J. Pharma. 538, 231 (2018).

[39] Y. Lia, H. Yanga, J. Yaoa, H. Yua, C. Xin, P. Zhanga, C. Xiao, Collo. Surf. B: Biointerfaces 169, 273 (2018).

[40] N. Iglesias, E. Galbis, M. J. Díaz-Blanco, M.-V. de-Paz, J.A. Galbis, Int. J. Pharm. 550 (1-2) 429 (2018).

[41] Y. Du, L. Ling, M. Ismail, W. He, Q. Xia, W. Zhou, C. Yao, X. Li, Int. J. Pharm. 549 (1-2) 352 (2018).

[42] P. Dramoua, M. Fizira, A. Taleb, A. Itatahinea, N.S. Dahirua, Y.A. Mehdi, W. Liu, J. Zhanga, H. Hea, Carbohydrate Polymers 197, 117 (2018).

[43] A. Deba, V.R. J. Drug Deliv. Sci. Techno. 43, 333 (2018).

[44] M. Bzowska, A. Karabasz, K. Szczepanowicz, Collo. Surf. A: Physicochem. Eng. Aspe.557, 36 (2018).

[45] M-M. Mayte, R-B. Guillermo, M. Bermejo, G-A. Isabel, G-A. Marta, V. Merino, Eur. J. Pharma. Biopharma. 136, 174 (2019).

[46] D. Zahn, A. Weidner, Z. Nosrati, L. Wöcke, J. Dellith, R. Müller, K. Saatchi, U.O. Häfeli, S. Dutz, J. Magnet. Magnet. Mater. 469, 698 (2019).

[47] W.T. Li, B.X. Xue, K. Shi, Y. Qu, B.Y. Chu, Z.Y. Qian, Appl. Mater. Today 14, 84 (2019).

[48] C-G. Alejandro, C-C. Elisa, R-B. Eva, V. Moreno, E. Fernández, P. Botella, J. Collo. Interface Sci. 541, 163 (2019).

[49] J.P. Quiñonesa, C.C. Mardareb, A.W. Hassel, O. Brüggemanna, Carbohydrate Polymers 206, 641 (2019).

[50] P. Costa, J.M. Sousa Lobo, Eu. J. Pharm. Sci. 13, 123 (2001).

[51] G. Singhvi, M. Singh, Int. J. Pharm. Stu. Res. 2, 1, 77 (2011).

[52] C. Salome, O. Godswill, O. Ikechukwu, Res. J. Pharm. Biol. Chem. Sci. 4,2, 97 (2013).

[53] G. Maria, A.L. Stoica, I. Luta, D. Stirbet, G.L. Radu, Microporous Mesoporous Mater. 162, 11, 80 (2012).

[54] G. Maria, I. Luta, Chem. Pap. 65, 4, 542 (2011).

[55] M.C. Thounaojam, R.N. Jadeja. M. Valodkar, P.S. Nagar, R.V. Devkar, S. Thakore, Food and chemical toxicology, 49, 2990 (2011).

[56] C.W. Zeng, X.J. Zhang, K.Y. Lin, H. Ye, S.Y. Feng, H. Zhang, Y.Q. Chen, Mole. Pharma. 81, 578 (2012).

[57] D. Madamwar, D.K. Patel, S.N. Desai, K.K. Upadhyay, R.V. Devkar, EXCLI Journal 14, 527 (2015).